P-ISSN 1991-8941
E-ISSN 2706-6703
Vol. 20, No. 1 (2026)

Journal of University of Anbar for Pure Science
(JUAPS)

journal homepage: juaps.uoanbar.edu.iq

Open Access

Original Paper

Study of pre-equilibrium contribution to total absorption cross section in some samarium isotopes using exciton model

Mariam A. Awad[1], **Nabeel F. Lattoofi**[1*]

[1]Department of Physics, College of Science, University of Anbar, Anbar, Iraq

ARTICLE INFO

Received: 19/06/2025
Accepted: 27/07/2025
Available online: 16/03/2026
April Issue
10.37652/juaps.2025.134412.1441

Cite @ JUAPS

Corresponding author
Nabeel F. Lattoofi
dr.nabeel.fawzi@uoanbar.edu.iq

ABSTRACT

Photonuclear reactions were studied for the samarium isotopes 144Sm, 148Sm, 150Sm, 152Sm, and 154Sm over an energy range of 8–22 MeV using the EMPIRE 3.2.2 nuclear reaction code. Total photoabsorption cross sections, particularly the Giant Dipole Resonance (GDR), were analyzed by considering contributions from both compound-nucleus and pre-equilibrium mechanisms. The Hauser–Feshbach model was employed to describe the compound-nucleus contribution, while the exciton model was used for the pre-equilibrium process. The results showed that the compound-nucleus mechanism is dominant across the studied energy range, although pre-equilibrium effects become more noticeable at higher energies. Furthermore, the influence of various gamma-ray strength function models, including MLO and EGLO, was evaluated. It was observed that different MLO variants yield consistent results, whereas the EGLO model fails to reproduce the double-peaked GDR structure characteristic of deformed samarium isotopes. These findings contribute to a better understanding of photonuclear reaction mechanisms and the applicability of gamma-ray strength function models in nuclear structure studies.

Keywords: *EMPIRE 3.2.2 code, Gamma strength function, Giant dipole resonance*

1 INTRODUCTION

Giant resonances (GRs) are high-frequency collective excitations in atomic nuclei, and their study reveals important information about nuclear properties. The isoscalar giant dipole resonance (GDR) is of particular interest because its energy is directly related to nuclear deformation; differences in oscillation frequencies along the major and minor axes can split the GDR [1, 2]. Giant dipole modes have been widely used to probe the properties of hot, rotating nuclei. For instance, the emergence of a double-peak structure in the photoabsorption spectrum of isotopes such as 152Sm indicates nuclear deformation [3]. Although deformation splitting is less noticeable for GRs with higher multipolarity, peak broadening has been observed in these cases as well, reflecting changes in the distribution of strength. By systematically studying GRs, unique insights into phase transitions in nuclear shapes can be gained. Unlike low-energy excitations, GRs provide a more direct reflection of the bulk properties of nuclear matter [4–6].

Nuclear reaction cross sections are consequential for various applications in astrophysics, nuclear energy, and national protection. When these cross sections cannot be measured directly or predicted reliably, indirect methods for determining the relevant reaction rates become necessary [7]. Nuclear reaction mechanisms are commonly separated into three types (direct, compound, and pre-equilibrium). A direct reaction is the first type, in which the incident particle interacts on a short timescale with a single proton and a single neutron, generally near the surface of the target nucleus. Furthermore, the time that a nucleon takes to cross the nucleus is short (about 10^{-22}), and this allows it to interact with only a small number of nucleons near the surface of certain nuclei.

Therefore, only a limited part of the target participates in the earliest stage of the interaction. Such reactions are typically forward-directed, unlike compound reactions, and are often discussed as the "reverse" limit of compound formation. Direct reactions remain a very active field in nuclear physics: they are used as experimental tools, as a playground for new ideas developed in nuclear reaction theory, and as direct probes of nuclear structure [8, 9].

Second, compound nucleus formation occurs when a large number of protons and neutrons are involved in a complex sequence of two-body reactions for a long enough time to create a relatively long-lived intermediate. In this case, thermal equilibrium is reached in the remaining system, and this type of mechanism is most prominent at low energies for the given target system. The cross section of this type varies strongly for small variations in the incident particle energy [10, 11]. The third type, pre-equilibrium, is an intermediate mechanism between direct and compound reactions. It occurs on a longer timescale than direct interaction but on a shorter timescale than compound-nucleus formation. This type is distinguished by an incident particle that continuously undergoes subsequent scattering. As scattering proceeds, increasingly complex states are created in the remaining system, and the information contained in the initial interaction is gradually lost. This interaction type is especially important when considering highly energetic incident particles; if the remaining system has sufficient excitation energy, the emission of subsequent particles may become more likely [12]. Pre-equilibrium processes are crucial mechanisms in nuclear reactions induced by light projectiles with incident energies above 10 MeV [13, 14].

The exciton model for nuclear reactions describes the full spectrum of reactions, ranging from very fast, direct reactions to relatively slow compound-nucleus processes [15]. The exciton model is a phenomenological description based on phase-space arguments, in which energy balance in a compound nucleus is treated in terms of the creation and destruction of pairs of particle–hole degrees of freedom [16]. It describes the reaction as a multistep process in which transitions occur between various classes of states. The exciton number, i.e., the number of excited particles and/or holes, characterizes these classes [17]. Griffin proposed the model in 1966 as a simple framework for describing diverse nuclear interactions in an energy range around 10 MeV, in which the incident particle shares its energy with the target nucleus in two-body collisions. These collisions increase the number of excitons by exciting particles above the target nucleus's Fermi sea and creating holes below it. Each state is treated statistically, allowing transitions to states with different exciton numbers or emission of particles into the continuum. The model and its modifications have been widely used in the analysis of excitation functions and particle energy spectra, and the results of these studies generally show good agreement between experimental and theoretical results [18, 19].

This model includes phenomenological parameters, but they are few and approximately constant over large mass and energy ranges, which has improved the understanding and practical description of nuclear reactions. It is appropriate for practical applications, especially for evaluating cross sections of neutron-induced reactions. It continues to be developed and has been used not only for predicting cross sections and energy spectra (including γ-ray competition) but also for angular distributions. One of the most important developments is the inclusion of explicit angular-momentum and parity conservation, with the requirement that the Hauser–Feshbach model be recovered as a limiting case [20].

Gamma-ray strength function (GSF) models are consequential in nuclear structure studies because they are essential ingredients in compound-nucleus calculations of capture cross sections, γ-ray spectra, and the competition between γ-ray and particle emission. They also provide average characterizations of electromagnetic properties of excited nuclei and characterize the average γ-decay behavior of a nucleus as a function of excitation energy. In addition, they contribute to statistical nuclear theory in astrophysics, reactor design, and waste transmutation, and they are used as tools applied in nuclear reaction model calculations [21, 22]. Gamma emission is a crucial channel for deexciting nuclei at energies below 1 MeV and accompanies most nuclear reactions. Accordingly, selecting an appropriate strength function is important for obtaining reliable calculated observables across diverse practical cases. Radiative strength functions (RSF) include two types that describe γ decay and photoabsorption: a downward intensity function that determines the average radiative width of γ decay, and an upward intensity function for photoexcitation that is associated with the cross section for absorbing a gamma ray [23].

In this study, the contributions of the compound nucleus and pre-equilibrium mechanisms to the total photoabsorption cross section were investigated using the Hauser–Feshbach and exciton models, respectively. The total cross sections for some samarium isotopes were

also studied using different gamma-strength functions. The default EMPIRE-specific level densities, adjusted to RIPL-3 experimental average neutron resonance spacings and to discrete levels, were used. A suitable optical potential model for the energy range and atomic number of the isotopes under study was also used [24]. These calculations, performed with the EMPIRE 3.2.2 code, were compared with available experimental data adopted from the EXFOR database.

2 MATERIALS AND METHODS

The cross-section of a photon that is absorbed by a nucleus can be calculated in EMPIRE and by using the nuclear code by using two unique nuclear reaction processes: the quasi-deuteron (QD) photo-absorption process and the giant dipole resonance (GDR) [25, 26]. The photo-absorption cross-section $\sigma_{abs}\ (E_\gamma\ )$ equation that is observed experimentally incorporates both of these two mechanisms, as shown below:

$$\sigma_{abs}\left(E_\gamma\right) = \sigma_{GDR}\left(E_\gamma\right) + \sigma_{QD}\left(E_\gamma\right) \tag{1}$$

The GDR cross section can be calculated by adding the contribution of the compound nucleus and preequilibrium cross sections. The basic feature of the compound nucleus model, as applied to photonuclear reactions, is that the nucleus is excited by the absorption of the photon via dipole interaction. After the absorption, a compound nucleus is formed, which subsequently deexcites by the evaporation of one or more particles.

In the Hauser-Feshbach model, the cross–section for the (a, b) reaction is expressed as follows [27]:

$$\sigma_{a,b}(E) = \sum_{J\pi} \sigma_a^{CN}(E, J\pi) P_b(E, J\pi) \tag{2}$$

Where $\sigma_a^{CN}(E, J\pi)$: The CN creation cross-section in a state characterized by spin and parity (J).$P_b(E, J\pi)$: The CN decay probability of a given energy Ex into the b channel.

In terms of transmission coefficients, the probability of decay:

$$P_b(E, J\pi) = \frac{T_b\left(E_x, J\pi\right)}{\sum_c T_c\left(E_x, J\pi\right)} \tag{3}$$

for p particle-emission:

$$T_p(E, J\pi) = \sum_{I=|J-j|}^{I=J+j} \int_0^{E_x - B_p} \sum_{lj} T_{p,lj}\left(E_x - B_p + \varepsilon\right) \rho\left(\varepsilon, I\pi_I\right) \delta\left(\pi\pi_l, (-1)^l\right) d\varepsilon \tag{4}$$

where $\rho\left(\varepsilon, I\pi_I\right)$ is the density of levels in the residual nucleus with the spin and parity I, π_I

$T_{p,lj}$ is the transmission coefficient having channel energy $\left(E_x - B_p + \varepsilon\right)$, and the orbital angular momentum 1 , which together with the particle spin s couples to the channel angular momentum j used to select in the residual nucleus spins I populated for a given compound nucleus spin J. $\delta\left(\pi\pi_I, (-1)^l\right)$ is the factor that stands for parity conservation.

For gamma (γ) decay, coefficient displays the similarly expression by:

$$T_\gamma\left(E_x, J\pi\right) = \sum_{xL} \sum_{J'=|J-j|}^{|J+j|} \int_0^{E_x} f_{xl}\left(\varepsilon_\gamma\right) \rho\left(E_x - \varepsilon_\gamma, J', \pi'\right) \delta\left(\pi\pi', (-1)^L\right) d\varepsilon_\gamma \tag{5}$$

where XL is defined as the photon type and multipole and $f_{xl}\left(\varepsilon_\gamma\right)$ is the Gamma-ray strength function.

Currently, the exciton model module PCROSS is used to calculate pre-equilibrium emission in photo-nuclear interactions: as the one-particle-one-hole excitation for the GDR fraction and as the two-proton-two-hole excitation for the QD fraction. However, this method does not account for the relationship of two holes that are created by the QD mechanism, which would necessitate a first shape that is nearer to a 2p1h one than a 2p2h one [28].

The exciton model of Kalbach has been used to calculate pre-equilibrium cross-sections for each particle that is emitted in binary reactions, as well as to calculate the compound nucleus cross-section for each binary reaction, besides the continuous level collections of residual nuclei that can increase the decay to calculate the corrections [29].

The basic assumption is that the intermediate states of the composite nucleus are characterized by a number called the exciton number n (or number of excited particles P and holes h) and by the excitation energy E. In general, for a given state and energy range, the probability of finding a particle is determined by the state densities. The density of the particle-hole state given by [18]

$$\omega(p, h, E) = g \frac{\left(gE - A_{p,h}\right)^{p+h-1}}{p!h!(p+h-1)!} \tag{6}$$

with g is the state density of single particle g = 6a/π2 in which a is the level density parameter in the equal

spacing model. $A_{p,h} = \frac{1}{4}\left(p^2 + h^2 + p - 3h\right)$ is the Pauli-exclusion first order correction effect.

The pre-compound reaction cross sections can be able to be calculate if the transition rates and particle decay rates are known, which are the transition rates of creating a particle-hole pair ($\Delta p = \Delta h = +1$), annihilating a particle-hole pair ($\Delta p = \Delta h = -1$), or simply by exciton-exciton scattering ($\Delta p = \Delta h = 0$), or undergo particle emissions with a certain decay width. These transition rates determined according to the first order time dependent perturbation theory as [30–32].

$$\lambda_+(p,h,E) = \frac{\Gamma_+(p,h,E)}{\hbar} = \frac{\pi}{\hbar}|M|^2 \frac{g}{(p+h+1)} \left(gE - C_{p+1,h+1}\right)^2 \quad (7)$$

$$\lambda_-(p,h,E) = \frac{\Gamma_-(p,h,E)}{\hbar} = \frac{\pi}{\hbar}|M|^2 gph(p+h-2) \quad (8)$$

$$\lambda_0(p,h,E) = \frac{\Gamma_0(p,h,E)}{\hbar} = \frac{\pi}{\hbar}|M|^2 g\left(gE - C_{p,h}\right) \times \left[\frac{p(p-1) + 4ph + h(h-1)}{P+h}\right] \quad (9)$$

where $C_{p,h} = \frac{1}{2}\left(p^2 + h^2\right)$ is the Pauli-exclusion first order correction effect. $|M|^2$ transition matrix element of two body $\left(|M|^2 = |M|^2_+ = |M|^2_- = |M|^2_0\right)$.Γ_+, Γ_-, and Γ_0 are the transition widths from the (p, h) state to (p + 1, h + 1), (p − 1, h − 1) states and remaining in a given (p, h) state, respectively. A general pre-equilibrium formulation of probability per unit time of a decay particle β with channel energy ϵ from a state with p particle and h hole is [15, 33–35]:

$$W_\beta\left(p,h,E,\epsilon_\beta\right) = \left[\frac{\omega\left(p - p_\beta, h, U\right)}{\omega(p,h,E)} R_\beta(p)\gamma_\beta\omega\left(p_\beta, 0, E-U\right)d\epsilon\right]\lambda^c_\beta(\epsilon) = \frac{2s_\beta+1}{\pi^2\hbar^3}\mu_\beta\sigma_\beta(\epsilon)\epsilon d\epsilon \times \frac{\omega\left(p-p_\beta,h,U\right)}{\omega(p,h,E)} \times \frac{\omega\left(p_\beta,0,E-U\right)}{g_\beta} R_\beta(p)\gamma_\beta \quad (10)$$

where s_β is the spin, μ_β reduced mass, and σ_β the inverse reaction cross section for the emitted particle β.U and E are the residual and composite nuclei excitation energies.

p_β is the number of particle emitted. $R_\beta(p)$, is the probability that of the outgoing particle β at p excited particles has the right combination of protons and neutrons and γ_β is the probability formation of particle β in the composite nucleus to have the right momentum to undergo emission as an entity. $\lambda^c_\beta(\epsilon)$ [15, 34] is the emission rate for a particle β at energy ϵ into the continuum:

$$\lambda^c_\beta(\epsilon) = \frac{\sigma_\beta(\epsilon)v_\beta p^c_\beta(\epsilon)}{g_\beta V} \quad (11)$$

where V is the laboratory volume, $v_\beta = \left(2\epsilon/\mu_\beta\right)^{\frac{1}{2}}$ is the β particle velocity with continuum state density $p^c_\beta(\epsilon) = \left(V/4\pi^2\hbar^3\right)\left(2s_\beta+1\right)\left(2\mu_\beta\right)^{3/2}\epsilon^{\frac{1}{2}}$ [15, 34]. The total decay probability per unit time for particle β from the (p, h) state i.e.,

$$\frac{\Gamma_\beta(p,h,E)}{\hbar} = \Lambda_\beta(p,h,E) = \int_0^{E-B} W_\beta(p,h,E,\epsilon)d\epsilon \quad (12)$$

where Bβ is the β-particle separation energy, $\Gamma_\beta(p,h,E)$ is total decay width for particle β at state (p, h). The total particle decay probability per unit time $\Lambda_c(p,h,E)$ is simply the sum over all possible decay channels, that is

$$\Lambda_c(p,h,E) = \frac{\Gamma_c(p,h,E)}{\hbar} = \sum_\nu \frac{\Gamma_\nu(p,h,E)}{\hbar} = \sum_\nu \Lambda_\nu(p,h,E) \quad (13)$$

ν includes contributions from particles such as neutrons (n), protons (p), deuterons (d), tritons (t), helium-3 (3He), and helium-4 (4 He). Based on equations (2) through (8), the total decay width of an intermediate exciton state characterized by (p, h) can be expressed as:

$$\Gamma(p,h,E) = \Gamma_+(p,h,E) + \Gamma_-(p,h,E) + \Gamma_c(p,h,E) \quad (14)$$

The mean lifetime associated with a specific (p, h) state is given by:

$$\tau(\mathrm{p},\ \mathrm{h},\mathrm{E}) = \frac{\hbar}{\Gamma(p,h,E)} = [\lambda_+(p,h,E) + \lambda_-(p,h,E) + \Lambda_c(p,h,E)]^{-1} \quad (15)$$

$\Gamma_+(p,h,E)/\Gamma(p,h,E), \Gamma_-(p,h,E)/\Gamma(p,h,E), \frac{\Gamma_c(p,h,E)}{\Gamma(p,h,E)}$ are the transition probabilities (or branching ratios) from

a given (p, h) state to the $(p+1, h+1)$ state, $(p-1, h-1)$ state, or to particle emission are defined, respectively, respectively. Under the "never come back" approximation, which neglects the Γ_-term, the probability of reaching any intermediate state starting from an initial state (p_0, h_0) is determined accordingly.

$$\mathrm{P(p,\ h, E)} = \prod_{\substack{p'=p \\ \Delta p\prime=+1}}^{p-1} \Gamma_+ \left(p', h', E\right) / \Gamma \left(p', h', E\right) \quad (16)$$

Where $p' - h' = p0 - h0$ and $P\left(p_0, h_0, E\right) = 1$. With this assumption, the pre-equilibrium decay probability for a particle β with energy between ϵ and $\epsilon + \mathrm{d}\epsilon$ can be obtained by summing from initial $(\mathrm{p_0},\ \mathrm{h_0})$ state to the most probable $(\bar{p}, \bar{h})$ state, that is

$$I_\beta^{PEQ}(E, \epsilon)d\epsilon = \sum_{\substack{p=p_0 \\ \Delta p=+1}}^{\bar{p}} \left[\frac{W_\beta\left(p, h, E, \epsilon_\beta\right)}{\Gamma_c(p, h, E)}\right] \left[\frac{\Gamma_c(p, h, E)}{\Gamma(p, h, E)}\right] \mathrm{P(p,\ h, E)} \quad (17)$$

or

$$I_\beta^{PEQ}(E, \epsilon)d\epsilon = \sum_{\substack{p=p_0 \\ \Delta p=+1}}^{\bar{p}} W_\beta(p, h, E, \epsilon)d\epsilon\tau_{PEQ}(\mathrm{p,\ h, E}) \quad (18)$$

with

$$\tau_{PEQ}(\mathrm{p,\ h, E}) = \frac{\hbar}{\Gamma(p, h, E)}\mathrm{P(p,\ h, E)} = \tau(\mathrm{p,\ h, E})\mathrm{P(p,\ h, E)} \quad (19)$$

where $\tau_{PEQ}(\mathrm{p, h, E})$ is the time spent by the composite nucleus in the (p, h) state at pre-equilibrium stage. Taking the contributions of "come back" into account, neglecting higher order contributions, the total pre-equilibrium decay probability with energy ϵ of a particle β [35]:

$$I_\beta^{PEQ}(E, \epsilon)d\epsilon = \sum_{\substack{p=p_0 \\ \Delta p=+1}}^{\bar{p}} \left[\frac{\Gamma_\beta(p, h, E, \epsilon)d\epsilon}{\Gamma_c(p, h, E)}\right] \left[\frac{\Gamma_c(p, h, E)}{\Gamma(p, h, E)}\right] \times \left[\prod_{\substack{p'=p \\ \Delta p\prime=+1}}^{p-1} \Gamma_+ \left(p', h', E\right) / \Gamma \left(p', h', E\right)\right] \times \left[1 + \frac{\Gamma_+(p, h, E)}{\Gamma(p, h, E)} \times \frac{\Gamma_-(p+1, h+1, E)}{\Gamma(p+1, h+1, E)}\right] \quad (20)$$

$\Gamma_\beta(p, h, E, \epsilon) = \hbar W_\beta(p, h, E, \epsilon)$ particle β width emission, and the time of the composite nucleus in a given p-h state:

$$\tau_{PEQ}(\mathrm{p,\ h, E})\tau(\mathrm{p,\ h, E})\mathrm{P(p,\ h, E)} \times \left[1 + \frac{\Gamma_+(p, h, E)}{\Gamma(p, h, E)} \times \frac{\Gamma_-(p+1, h+1, E)}{\Gamma(p+1, h+1, E)}\right] \quad (21)$$

Then the pre-equilibrium emissions fraction is:

$$F_{PEQ}^E = \sum_\nu \int_0^{E-B_\nu} I_\nu^{PEQ}(E, \epsilon)d\epsilon = \sum_{\substack{p=p_0 \\ \Delta p=+1}}^{\bar{p}} \Lambda_c(p, h, E)\tau_{PEQ}(\mathrm{p,\ h, E}) \quad (22)$$

with $F_{EQ}(\mathrm{E}) = 1 - F_{PEQ}(E)$.

The photonuclear reaction energy spectrum for pre-equilibrium stage:

$$\frac{d\sigma_\beta^{PEQ}\left(E_\gamma\right)}{d\epsilon} = \sigma_a\left(E_\gamma\right) I_\beta^{PEQ}\left(E_\gamma, \epsilon\right)$$

The gamma decay intensity function that limits the average radiative width of the gamma-decay for gamma-ray emission of multi-pole sort XL is identified as [27]:

$$\overleftarrow{f}_{XL}\left(E_\gamma\right) = \frac{E_\gamma^{-(2L+1)}\left\langle\Gamma_{XL}\left(E_\gamma\right)\right\rangle}{D_l} \quad (23)$$

with ${E_\gamma}^{-(2L+1)}\left\langle\Gamma_{XL}\left(E_\gamma\right)\right\rangle$ is the average reduced partial radiation width, D_l is the average level spacing, and E_γ is the gamma-ray energy [23]. Photo-absorption cross-section of dipole γ-ray with energy (E γ) by non-deformed cold nucleus as an example of the radiative strength functions (RSF) is proportional to the (RSF) of photo-absorption operation $\vec{f}\left(E_\gamma\right)$ where (RSF) is an essential component of the statistical theory of nuclear interactions by the relation [36]:

$$\sigma\left(E_\gamma\right) = 3(\pi\hbar c)^2 E_\gamma \vec{f}\left(E_\gamma\right) \quad (24)$$

The photo-excitation strength function $\vec{f}_{EL}$ is linked to the cross-section for γ-ray absorption and is limited by the average of $\left\langle\sigma_{XL}\left(E_\gamma\right)\right\rangle$ summarized overall probable spins of the last states:

$$\vec{f}_{EL}\left(E_\gamma\right) = \frac{E_\gamma^{-(2L+1)}}{(\pi\hbar c)^2}\frac{\left\langle\sigma_{XL}\left(E_\gamma\right)\right\rangle}{2L+1} \quad (25)$$

Lorentzian parameters of (GRs) are essential to calculate gamma-ray strength functions with closed-shape models [23, 37, 38]. The emission and absorption of dipole gamma rays from atomic nuclei in the energy region up to E$\gamma \approx$ 20MeV is principally governed by the excitation of the isovector giant dipole resonance (IVGDR). The brink hypothesis in the standard Lorentzian model (SLO) has been widely used to compute dipole gamma-ray strength. The dipole radiative strength function in this model is a singular Lorentzian for non-deformed nuclei with an energy autonomous width (Γ) that is taken to be equivalent to the GDR width Γr :

$$\overleftarrow{f}\left(E_\gamma\right) = \vec{f}\left(E_\gamma\right) \equiv f_{SLO}\left(E_\gamma\right) = 8.674.10^{-8} \times \sigma_r \Gamma_r \frac{E_\gamma \Gamma_r}{\left(E_\gamma^2 - E_r^2\right)^2 + \left(E_\gamma \Gamma_r\right)^2} \quad (26)$$

The enhanced Generalized Lorentzian model (EGLO) for non-deformed nuclei includes two ingredients and the following:

$$\vec{f}_{EGLO}\left(E_\gamma\right) = 8.674.10^{-8} \times \sigma_r \Gamma_r \times \left[\frac{E_\gamma \Gamma_k\left(E_\gamma, T_f\right)}{\left(E_\gamma^2 - E_r^2\right)^2 + \left(E_\gamma \Gamma_k\left(E_\gamma, T_f\right)\right)^2} + 0.7\Gamma_k\left(E_\gamma = \frac{0, T_i}{E_r^3}\right)\right] \quad (27)$$

where Ti (Tf) is the temperature of the first (last) states. The GFL dipole strength function in non-deformed nuclei is well-identified as:

$$\overleftarrow{f}\left(E_\gamma\right) = \overleftarrow{f}_{GFL}\left(E_\gamma\right) = 8.674.10^{-8} \times \sigma_r \Gamma_r K_{GFL} \frac{E_\gamma \Gamma_m\left(E_\gamma, T_f\right)}{\left(E_\gamma^2 - E_r^2\right)^2 + K_{GFL} {E_\gamma}^2 \left(\Gamma_m\left(E_\gamma, T_f\right)\right)^2} \quad (28)$$

where $K_{GFL}\Gamma_m {E_\gamma}^2$ has been included in the denominator to prevent the GFL approach's singularity around the GDR energy. K_{GFL} is the factor involved in maintaining the standard correlation between the strength function at the GDR energy and the hump value of or. The expression for the dipole gamma-ray strength function with the MLO model $\overleftarrow{f}\left(E_1\right) \equiv \overleftarrow{f}_{MLO}\left(E_\gamma\right)$) is obtained by computing the average radiative width of nuclei with microcanonically distributed first states where the function has the next shape for non-deformed nuclei

$$\overleftarrow{f}\left(E_\gamma\right) = \overleftarrow{f}_{MLO}\left(E_\gamma\right) = 8.674.10^{-8} \times \Lambda\left(E_\gamma, T_f\right) \sigma_r \Gamma_r \frac{E_\gamma \Gamma\left(E_\gamma, T_f\right)}{\left(E_\gamma^2 - E_r^2\right)^2 + {E_\gamma}^2 \left(\Gamma\left(E_\gamma, T_f\right)\right)^2} \quad (29)$$

where $\Gamma\left(E_\gamma, T_f\right)$ is the strength function width dependent on the temperature (T_f) of the last state, and the gamma-ray energy [23].

3 RESULTS AND DISCUSSION

The total giant dipole resonance (GDR) cross sections for the 144,148,150,152,154Sm isotopes were first calculated by adding the contributions from different nuclear reaction models and then compared with the experimental data within the studied energy range. At the same time, the effect of gamma-ray strength functions on these total cross sections was investigated to identify the function that best agrees with the experimental data. Figure 1a-e illustrates the total cross sections for the isotopes under study with experimental data points compared to the theoretical contributions from different reaction components. It can be observed that the computed GDRs for all Sm isotopes reproduce the form of the GDR cross section perfectly. The theoretical total GDR cross section, which includes all contributions and is shown as the solid black curve, was fitted to align with the experimental data and represents the overall behavior of the resonance. The pre-equilibrium and compound nucleus contributions, labeled with red and black curves, are also shown in this figure. The pre-equilibrium contribution arises from nucleons that do not fully equilibrate before emission and is relatively small compared with the compound nucleus contribution, which is the dominant process within the GDR energy range and follows the characteristic GDR shape. It becomes more noticeable at higher energies, especially in the second peak for the deformed 152,154Sm nuclei, and may provide a subtle enhancement to the overall cross section, yielding excellent agreement with the experimental one.

The shape of the total GDR curve reflects the overlap of different oscillation frequencies along the two principal axes of the nucleus, resulting in a broader resonance than in spherical nuclei and two or more resonance peaks in deformed nuclei. These two peaks, with different energies, correspond to nucleon oscillations along the long (low-energy) and short (higher-energy) axes, respectively, and reflect prolate or oblate deformation.

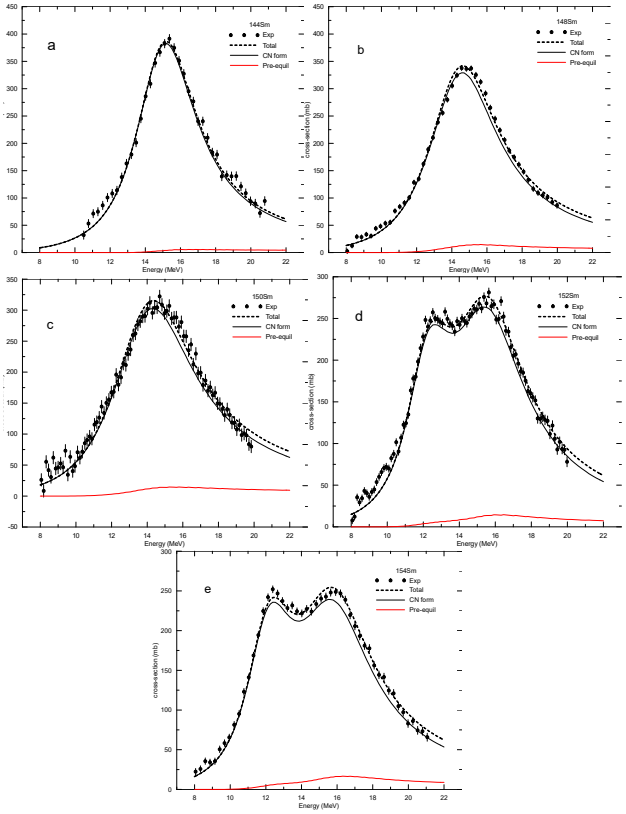

Fig. 1 Giant dipole resonance cross section and its contributions for samarium isotopes (a) for ^{144}Sm, (b) for ^{148}Sm, (c) for ^{150}Sm, (d) for ^{152}Sm, and (e) for ^{154}Sm along with experimental data

The compound nucleus contributions for the samarium isotopes are shown in Figure 2. These calculations were performed using the Hauser–Feshbach statistical model, which assumes that a compound nucleus is formed following photon absorption and subsequently decays via particle emission. The compound nucleus contribution decreases with increasing mass number and follows the characteristic GDR shape. This reveals an inverse relationship between the compound cross section and nuclear deformation: more spherical isotopes (e.g., 144Sm) exhibit higher compound nucleus cross sections, with peak values exceeding 350 mb, whereas more deformed isotopes (e.g., 152Sm and 154Sm) peak at noticeably lower values (≈250 mb and below).

This behavior can be interpreted within the Hauser–Feshbach framework. In more spherical nuclei, the reaction flux proceeds predominantly through compound nucleus formation, yielding a stronger compound contribution. In more deformed nuclei, the higher-level density and the increased number of accessible configurations facilitate faster dissipation through non-equilibrium pathways, thereby reducing the fraction of reactions that proceed via full compound nucleus formation and lowering the compound contribution.

The onset of a significant compound cross section appears similar across all isotopes (≈10 MeV), whereas the resonance width and peak position show only minor variation. The more spherical 144Sm shows a sharper and higher peak, while the more deformed isotopes exhibit broader but lower peaks. Overall, as the mass number increases from 144Sm to 154Sm, the compound nucleus contribution decreases, opposite to the trend observed for the pre-equilibrium mechanism.

Figure 3 presents the pre-equilibrium reaction cross sections for the samarium isotopes under study as a function of incident γ-ray energy, calculated using the exciton model implemented in the PCROSS subroutine [27]. The results highlight the contribution of pre-equilibrium processes within the GDR region (8–22 MeV) and the effects of nuclear deformation and mass number on the cross-section behavior. Nuclear deformation clearly enhances the pre-equilibrium γ-induced reaction mechanism. Deformed isotopes, such as 152Sm and 154Sm, exhibit higher and broader pre-equilibrium peaks than the more spherical 144Sm. This behavior is consistent with the higher level density in deformed nuclei, which increases the number of available intermediate exciton configurations. In Griffin's exciton model [39], the pre-equilibrium stage evolves through successive two-body interactions within the composite nucleus; deformation facilitates access to higher-order particle-hole states, increasing the emission probability before statistical equilibrium is reached.

In addition, the energy threshold for noticeable pre-equilibrium emission is lower for the more deformed isotopes. For example, 154Sm and 152Sm begin to show clear pre-equilibrium contributions around 9–10 MeV, whereas the more spherical 144Sm shows a delayed onset near 11 MeV. This may reflect stronger coupling between the γ-ray field and collective dipole modes in deformed nuclei, which can favor earlier non-equilibrium emission.

A further observation is the increase in the peak pre-equilibrium cross section with increasing mass number. Heavier isotopes, such as 154Sm, exhibit larger magnitudes and a slight shift of the pre-equilibrium peak toward higher photon energies. While this trend also tracks the increase in atomic number, it is likely dominated by the larger quadrupole deformation (β_2) in heavier samarium isotopes, which enhances level density and

dipole response. Overall, these results support the exciton model's sensitivity to nuclear-structure effects, especially deformation and mass number. As implemented in PCROSS and EMPIRE, the model describes the transition from initial dipole excitation to particle emission through non-equilibrium pathways and provides a consistent explanation for the isotope-dependent behavior of photonuclear reactions in the GDR region.

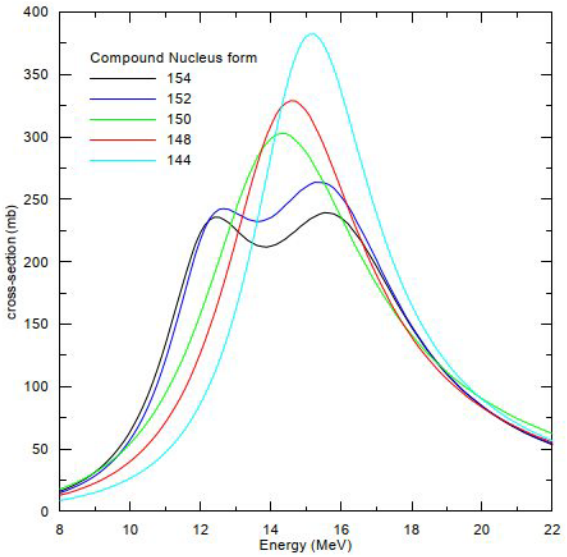

Fig. 2 The compound nucleus reaction cross-section for Sm isotopes

Figure 4a, b, c, d, and e display the calculation of the GDR cross-section for samarium isotope based on various gamma-ray strength functions, which differ in their treatment of nuclear deformation, damping mechanisms, and resonance parameters. The results were overlaid with the experimental data and then compared across the different strength-function options. The modified Lorentzian (MLO) models incorporate temperature and deformation effects and aim to describe both the GDR peak region and the high-energy tail. Variations among MLO parametrizations introduce refinements such as additional energy- or temperature-dependent terms, which can improve agreement over a broader energy range and better reflect the GDR splitting observed in deformed nuclei.

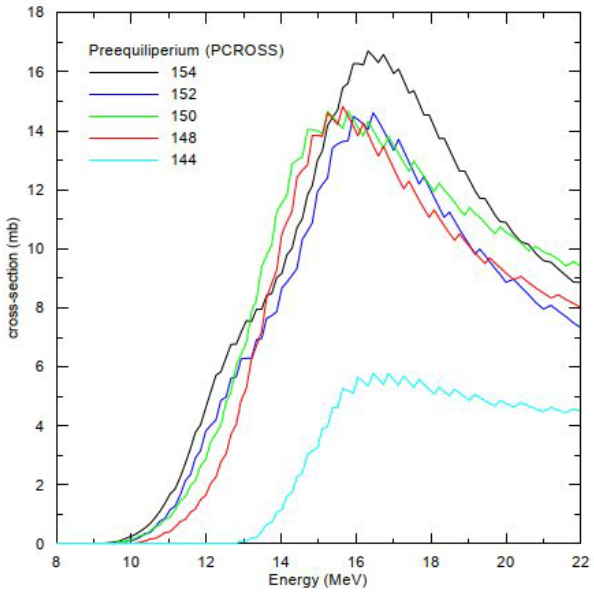

Fig. 3 The pre-equilibrium reaction cross-section for Sm isotopes

The standard Lorentzian (SLO) model is closer to a global Lorentzian description, typically implemented with deformation corrections, but it is generally less flexible at reproducing the peak and tail simultaneously.

EGLO (RIPL) is an enhanced generalized Lorentzian formulation tuned to the Reference Input Parameter Library (RIPL) and is often adopted for practical calculations in deformed nuclei. It includes an energy-dependent width and a damping mechanism that helps capture the spreading of the strength function at lower energies; accordingly, it can better reproduce the experimental low-energy behavior when temperature effects become relevant in an excited nucleus. The generalized Fermi liquid (GFL) approach also considers deformation, but it differs in how the resonance is parametrized and, in its simpler treatment, can miss deformation effects. As a result, it typically provides intermediate agreement, capturing some aspects of the resonance, while lacking precision in the tail or peak regions and sometimes underestimating the resonance-peak cross section. In contrast, the EGLO (Uhl–Kopecky) option fails to reproduce the broader GDR shape and tends to overestimate the peak cross section because deformation is not treated adequately [40].

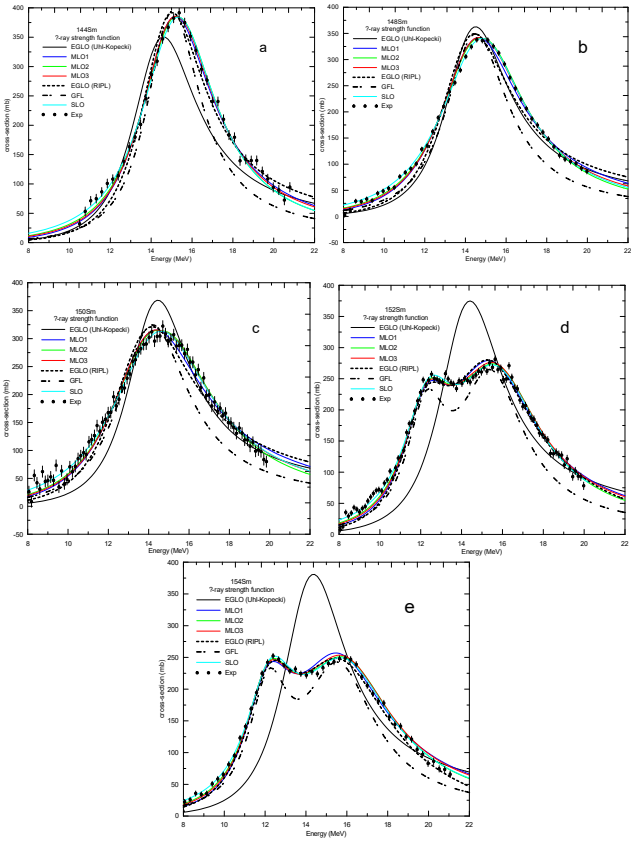

Fig. 4 The total cross-section for Sm isotopes calculated with different Gamma strength functions

The variation in the cross-section behavior across Sm isotopes is not solely quantitative; it also reflects deeper structural differences associated with nuclear deformation. One of the most important deformation effects on the GDR is the splitting of the resonance into two distinct components. This splitting arises from anisotropic oscillations of protons against neutrons along different nuclear axes in deformed nuclei. In a spherical nucleus, the GDR exhibits a single peak because the oscillation frequencies are identical along all axes. In contrast, in axially deformed nuclei (prolate or oblate), the resonance separates into two modes, associated with oscillations along the short and long axes. In practice, the split peaks correspond to different oscillation frequencies, and their overlap broadens the overall response compared to spherical nuclei. The resulting double-humped structure reflects the distribution of photoabsorption strength over a wider energy range.

Physically, the energy separation between the split GDR peaks is directly connected to the nuclear moment of inertia and the quadrupole deformation parameter (β_2). Greater deformation increases the asymmetry in the restoring force for proton–neutron oscillations, which in turn increases the GDR splitting. For example, 152Sm and 154Sm, known to have significant prolate deformation ($\beta_2 \approx 0.3 - 0.35$), show broader and flatter cross-section peaks compared with 144Sm, which is nearly spherical ($\beta_2 \approx 0.0$). This behavior is consistent with theoretical predictions based on hydrodynamic models and collective excitations.

Moreover, the position and width of the GDR peaks offer indirect insight into temperature-dependent shape evolution. At finite excitation energy, the nucleus may undergo shape changes (e.g., spherical-to-deformed) or experience enhanced surface vibrations. The broader response observed in heavier, more deformed Sm isotopes might therefore also reflect finite-temperature effects, where the nuclear shape fluctuates around an average deformed configuration. Overall, the observed GDR splitting and the corresponding cross-section profiles across the Sm isotopic chain not only quantify reaction mechanisms but also encode information about the underlying nuclear shape, the deformation energy surface, and collective motion at finite excitation. Correlating these features with known deformation parameters highlights the structural sensitivity of photonuclear reactions and supports their use as a spectroscopy tool for probing deformation systematics across isotopes.

4 CONCLUSION

The theoretical components combine to describe the total GDR, emphasizing the dominant role of the compound nucleus while accounting for the smaller pre-equilibrium process, which becomes more noticeable at higher excitation energies. The compound nucleus contribution captures deformation-induced splitting and closely follows the experimental data, indicating that deformation effects are properly reflected in the broadening and splitting of the GDR. The compound mechanism accounts for most of the cross-section, whereas the pre-equilibrium component contributes mainly to the high-energy side. Deformation might also slightly influence pre-equilibrium emission, because nuclear-surface geometry can affect particle-emission probabilities and, in turn, the total theoretical cross section.

The calculations also highlight the sensitivity of the computed GDR cross section to the selected gamma-ray strength function. Including deformation and energy-dependent effects generally improves agreement with

experimental data. The splitting produces a broader resonance with a two-component shape, which is well captured by most strength functions, except the simpler models (GFL). This comparison is important for selecting appropriate models for accurate predictions across different samarium isotopes.

Acknowledgement

N/A

Funding source

No funds received.

Data availability

N/A

DECLARATIONS

Conflict of interest

The authors declare no competing interests.

Consent to publish

N/A

Ethical approval

N/A

REFERENCES

[1] Capote R, Herman M, Obložinský P, Young PG, Goriely S, Belgya T, et al. RIPL – erence Input Parameter Library for Calculation of Nuclear Reactions and Nuclear Data Evaluations. Nuclear Data Sheets. 2009;110(12):3107–3214. 10.1016/j.nds.2009.10.004

[2] Blaizot JP. Nuclear compressibilities. Physics Reports. 1980;64(4):171–248. 10.1016/0370-1573(80)90001-0

[3] Camera F. Gamma decay of the giant dipole resonance and feeding of superdeformed states in 143Eu. Physics of Atomic Nuclei. 2001 jun;64(6):1039–1043. 10.1134/1.1383613

[4] Yoshida K, Nakatsukasa T. Shape evolution of giant resonances in Nd and Sm isotopes. Physical Review C. 2013;88(3). 10.1103/physrevc.88.034309

[5] Harakeh MN, Woude A. Giant Resonances: fundamental high-frequency modes of nuclear excitation. vol. 24. Oxford Studies in Nuclear Phys; 2001

[6] Bohr A, Mottelson BR. Nuclear Structure (2 vols.). World Scientific; 1998.

[7] Escher JE, Harke JT, Dietrich FS, Scielzo ND, Thompson IJ, Younes W. Compound-nuclear reaction cross sections from surrogate measurements. Reviews of Modern Physics. 2012;84(1):353–397. 10.1103/revmodphys.84.353

[8] Bertulani CA, Bonaccorso A. In: Direct Nuclear Reactions. Springer Nature Singapore; 2023. p. 1415–1449. 10.1007/978-981-19-6345-2_3

[9] Kamel DT, Lattoofi NF. Nuclear Level Density Effect for Induced Fission Cross-section Reactions on Some Even and Odd-A Americium Nuclei. Brazilian Journal of Physics. 2023;54(1). 10.1007/s13538-023-01395-6

[10] Mumpower MR, Neudecker D, Sasaki H, Kawano T, Lovell AE, Herman MW, et al. Collective enhancement in the exciton model. Physical Review C. 2023;107(3). 10.1103/physrevc.107.034606

[11] Loveland WD. Compound nuclear reactions. Journal of Chemical Education. 1972;49(8):529. 10.1021/ed049p529

[12] Gruppelaar H, Nagel P, Hodgson PE. Pre-equilibrium processes in nuclear reaction theory: the state of the art and beyond. La Rivista Del Nuovo Cimento Series 3. 1986;9(7):1–46. 10.1007/bf02725961

[13] BALDIK R, AYTEKIN H, TEL E. Equilibrium and pre-equilibrium calculations of cross-sections of (p, xn) reactions on 89 Y, 90 Zr and 94 Mo targets used for the production of 89 Zr, 90 Nb and 94 Tc positron-emitting radionuclides. Pramana. 2013;80(2):251–261. 10.1007/s12043-012-0472-5

[14] Lattoofi NF, Alzubadi AA. Study of giant dipole resonances for neodymium isotopes with an exciton model. International Journal of Modern Physics E. 2020;29(10):2050084. 10.1142/s0218301320500846

[15] Cline CK. Extensions to the pre-equilibrium statistical model and a study of complex particle emission. Nuclear Physics A. 1972;193(2):417–437. 10.1016/0375-9474(72)90330-2

[16] Kalbach C. Surface effects in the exciton model of preequilibrium nuclear reactions. Physical Review C. 1985;32(4):1157–1168. 10.1103/physrevc.32.1157

[17] Dobeš J, Běták E. Two-component exciton model. Zeitschrift für Physik A Atoms and Nuclei. 1983;310(4):329–338. 10.1007/bf01419519

[18] Ribanský I, Obložinský P, Běták E. Pre-equilibrium decay and the exciton model. Nuclear Physics A. 1973;205(3):545–560. 10.1016/0375-9474(73)90705-7

[19] Gupta SK. Two-component equilibration in the exciton model of nuclear reactions. Zeitschrift f r Physik A Atoms and Nuclei. 1981;303(4):329–333. 10.1007/bf01421531

[20] Gruppelaar H, Akkermans JM, et al. Recent developments in exciton and unified models. 1988

[21] von Neumann-Cosel P, Bassauer S, Martin D, Tamii A. Gamma Strength Functions and Level Densities from High-Resolution Proton Scattering under 0°. EPJ Web of Conferences. 2018;178:06002. 10.1051/epjconf/201817806002

[22] Kopecky J, Uhl M. Test of gamma-ray strength functions in nuclear reaction model calculations. Physical Review C. 1990;41(5):1941–1955. 10.1103/physrevc.41.1941

[23] Belgya T, Bersillon O, Capote R, Fukahori T, Zhigang G, Goriely S, et al. Handbook for calculations of nuclear reaction data, RIPL-2. IAEA, Vienna, Austria. 2006

[24] Koning AJ, Delaroche JP. Local and global nucleon optical models from 1 keV to 200 MeV. Nuclear Physics A. 2003;713(3–4):231–310. 10.1016/s0375-9474(02)01321-0

[25] Levinger JS. The High Energy Nuclear Photoeffect. Physical Review. 1951;84(1):43–51. 10.1103/physrev.84.43

[26] Levinger JS. Modified quasi-deutron model. Physics Letters B. 1979;82(2):181–182. 10.1016/0370-2693(79)90730-5

[27] Herman M, Capote R, Sin M, Trkov A, Carlson B, Obložinskỳ P, et al. EMPIRE-3.2 Malta: modular system for nuclear reaction calculations and nuclear data evaluation [User's Manual]. IAEA/OSTI record; 2013. 10.2172/1108585

[28] Chadwick MB, Young PG, MacFarlane RE, White MC, Little RC. Photonuclear Physics in Radiation Transport—I: Cross Sections and Spectra. Nuclear Science and Engineering. 2003;144(2):157–173. 10.13182/nse144-157

[29] Young P, Arthur ED, Chadwick M, et al. Comprehensive nuclear model calculations: introduction to the theory and use of the GNASH code. Los Alamos National Lab., NM (United States); 1992.

[30] Williams FC. Intermediate state transition rates in the Griffin model. Physics Letters B. 1970;31(4):184–186. 10.1016/0370-2693(70)90097-3

[31] Bemis CE, McGowan FK, Ford JLC, Milner WT, Stelson PH, Robinson RL. E2 and E4 transition moments and equilibrium deformations in the actinide nuclei. Physical Review C. 1973;8(4):1466–1480. 10.1103/physrevc.8.1466

[32] Obložinský P, Ribanský I, Běták E. Intermediate-state transition rates in the exciton model. Nuclear Physics A. 1974;226(2):347–364. 10.1016/0375-9474(74)90410-2

[33] Blann M. A priori pre-equilibrium decay models. Nuclear Physics A. 1973;213(3):570–588. 10.1016/0375-9474(73)90753-7

[34] Wu JR, Chang CC. Pre-equilibrium particle decay in the photonuclear reactions. Physical Review C. 1977;16(5):1812–1824. 10.1103/physrevc.16.1812

[35] Wu JR, Chang CC. Pre-equilibrium decay in the exciton model. Physics Letters B. 1976;60(5):423–426. 10.1016/0370-2693(76)90697-3

[36] PLUJKO VA, KADENKO IM, BEZSHYYKO OA, GOLINKA-BEZSHYYKO LO, DAVIDOVSKAYA OI. COMPARISON AND TESTING OF METHODS FOR E1 STRENGTH CALCULATIONS. International Journal of Modern Physics E. 2006;15(02):387–392. 10.1142/s0218301306004259

[37] Plujko VA. Implantation and Testing of Photonuclear Channel in Code EMPIRE II. In: AIP Conference Proceedings. vol. 769. AIP; 2005. p. 1108–1111. 10.1063/1.1945201

[38] Plujko VA, Ezhov SN, Kavatsyuk MO, Grebenyuk AA, Yermolenko RV. Testing and Improvements of Gamma-Ray Strength Functions for Nuclear Model Calculations. Journal of Nuclear Science and Technology. 2002;39(sup2):811–814. 10.1080/00223131.2002.10875222

[39] Griffin JJ. Statistical Model of Intermediate Structure. Physical Review Letters. 1966;17(9):478–481. 10.1103/physrevlett.17.478

[40] Plujko V, Kadenko I, Goriely S, Kulich E, Davidovskaya O, Gorbachenko O. Models for photoabsorption cross section estimates. In: ND2007. EDP Sciences; 2007. 10.1051/ndata:07731

How to cite this article

Awad MA, Lattoofi NF. Study of pre-equilibrium contribution to total absorption cross section in some samarium isotopes using exciton model . Journal of University of Anbar for Pure Science. 2026; 20(1):210-221. doi:10.37652/juaps.2025.134412.1441